

General Disclaimer

One or more of the Following Statements may affect this Document

- This document has been reproduced from the best copy furnished by the organizational source. It is being released in the interest of making available as much information as possible.
- This document may contain data, which exceeds the sheet parameters. It was furnished in this condition by the organizational source and is the best copy available.
- This document may contain tone-on-tone or color graphs, charts and/or pictures, which have been reproduced in black and white.
- This document is paginated as submitted by the original source.
- Portions of this document are not fully legible due to the historical nature of some of the material. However, it is the best reproduction available from the original submission.

ORIGINAL PAGE IS
OF POOR QUALITY.

9950-809

DOE/JPL-956046-82/X 5
Distribution Category UC-63

THE STRUCTURE OF <110> TILT BOUNDARIES
IN LARGE AREA SOLAR SILICON.

Annual Report

Period: August 31, 1981 to September 1982

JPL Contract No. 956046, Report #X.5.

Prepared by:

Dieter G. Ast
Principal Investigator

Dieter G. Ast

Department of Materials Science and Engineering
Cornell University
Ithaca, NY 14853.

December 1982



The JPL Flat Plate Solar Array Project is sponsored by the U.S. Department of Energy and forms part of the Solar Photovoltaic Conversion Program to initiate a major effort towards the development of low-cost solar arrays. This work was performed for the Jet Propulsion Laboratory, California Institute of Technology by agreement between NASA and DOE.

(NASA-CR-170204) THE STRUCTURE OF > 110 <
TILT BOUNDARIES IN LARGE AREA SOLAR SILICON
Annual Report, 31 Aug. 1981 - Sep. 1982
(Cornell Univ., Ithaca, N. Y.) 24 p
HC A02/MF A01

N 83-22744

Unclass
CSCL 10A G3/44 03419

THE STRUCTURE OF <110> TILT BOUNDARIES IN LARGE AREA SOLAR SILICON

D.G. Anter, R. Cunningham, and M. Vendin

Introduction

Most grain boundaries in polycrystalline silicon are tilt boundaries. Determination of the orientation relationship required to classify adjacent grains in terms of topographic correspondence, one distinguishes first, second, and third order twin boundaries. Thus, two grains which are related by a mirror operation across a (111) plane are first order or coherent twins. Grains related by two mirror operations, e.g. across (111) followed by a mirror operation across (111) are classified as second order twins etc.

Small deviations from the "ideal" first and higher twin orientations are taken up in analogy to the familiar case of small angle grain boundaries by periodic arrays of dislocations in the boundary plane. These dislocations are called boundary dislocations (displacement shift complete) dislocations of the boundary. The burgers vectors of these dislocations is generally much smaller than the burgers vectors of lattice dislocations.

Many of the concepts required to analyze the atomic structure of second and third order twin boundaries in silicon were introduced by

Hornstra in his papers on the structure of dislocations (1) and $\langle 110 \rangle$ tilt boundaries (2) in the diamond lattice. When modelling a lattice defect, Hornstra's criterion was to preserve tetrahedral bonding where possible, thereby minimizing the number of broken bonds. Radial distribution functions of amorphous silicon show that the Si-Si bonds vary in length by less than 1% from those in crystalline silicon, but that the bond angles can fluctuate by up to 15° (3). Therefore, an approach that minimizes the number of broken bonds and keeps the interatomic distances essentially fixed, whilst allowing bond angle variation, should produce relatively low energy configurations. Stick and ball models of five and seven membered rings of silicon atoms can be constructed without large strains, and Hornstra (1) proposed that a symmetrical combination of one five and one seven membered ring would form the core of an $a/2\langle 110 \rangle$ edge dislocation in the diamond lattice.

figure 1. Tilt boundaries with a $\langle 110 \rangle$ tilt axis and a $\langle 110 \rangle$ grain boundary plane in the median lattice (4) could be modelled as an arrangement of edge dislocations in combination with chair and boat shaped six membered rings (2). The Si-Si bonds in chair shaped rings are arranged in staggered configurations, whereas the boat shaped rings contain two pairs of eclipsed bonds. Hornstra considered $\langle 110 \rangle$ tilt boundaries where the rotation angle θ corresponded to a high coincidence (low Σ) misorientation, and modelled each boundary as a combination of a small number of identical structural units. Σ is the ratio of atom sites to coincidence sites (5). Hornstra's model for the $\{331\}\Sigma=19$, 26.53° boundary, figure 2, has the highest misorientation angle that can be accommodated by discrete $a/2\langle 110 \rangle$ edge dislocations. He developed two models for the $\{221\}\Sigma=9$, 38.94° boundary, which Kohn (6) has termed a second order twin boundary. The

first of the models contains adjoining $a/2\langle 110 \rangle$ edge dislocations arranged in a zig-zag fashion, figure 3(a). The alternative model, figure 3(b), consists of a regular array of $a\langle 110 \rangle$ dislocations created by interposing a six membered ring between the five and seven membered rings of the $a/2\langle 110 \rangle$ dislocation structure. Hornstra stated, without constructing a model, that the $(552)\Sigma=27$, 31.59° third order twin boundary could be built up from elements of the $\Sigma=19$ structure and either of the two $\Sigma=9$ structures. At that time (1958) no experimental evidence was available to decide which of the $\Sigma=9$ and $\Sigma=27$ models was more likely to be correct.

In this paper the models of Hornstra and their connection to the repeating group description of grain boundaries (7-10) are discussed. A model for the $\Sigma=27$ boundary containing a zig-zag arrangement of dislocations is constructed and it is shown that zig-zag models can account for the contrast features observed in high resolution transmission electron micrographs of second and third order twin boundaries in silicon. The boundaries discussed are symmetric with a $[1\bar{1}0]$ tilt axis and a (110) boundary plane in the median lattice (the median plane). The median lattice is identical in structure and halfway in orientation between the crystal lattices either side of the boundary. It is denoted by the subscript m.

Experimental Details

Silicon ribbon was produced by chemical vapor deposition at a temperature of 1100°C (11). The ribbons were polycrystalline with a predominantly $\langle 110 \rangle$ texture and an average grain size of about 1 μm .

TEM specimens were prepared by mechanically polishing the silicon to a thickness of about 75 μm , followed by ion beam milling. High resolution electron microscopy observations were carried out on a Siemens Elmiskop 102 operating at an accelerating voltage of 125kV. The $\langle 110 \rangle$ tilt boundaries were viewed end-on, with the incident beam parallel to the tilt axis. Lattice images were recorded with the inner seven beams from the $\langle 110 \rangle$ zone of each crystal included in the objective aperture.

Results

Figure 4 is a lattice fringe image of a $[110]$ tilt boundary imaged parallel to the tilt axis. The boundary exhibits faceting on a scale of about 10nm and also appears faceted at the atomic level. The crystallography is shown in figure 4 with subscripts to indicate the crystal to which a plane or vector refers. The long facet marked X is a $(552)_1/(552)_2$ symmetric third order twin boundary, median plane (110) . This plane contains the second highest density of coincidence sites for the $\Sigma=27$ misorientation. The plane with the highest density of coincidence sites for the $\Sigma=27$ misorientation is $(115)_1$ (median plane (001)) which is orthogonal to the plane of the observed boundary. In the boundary shown in figure 4, a pattern of four large white dots repeats every 2.80nm. A line can be drawn through these white dots that is faceted on two planes, $(111)_1$ and $(11\bar{1})_2$, and the two white dots in each facet plane differ in size. The boundary changes direction and character at Y, dissociating into a coherent first order twin boundary (arrowed) and a symmetric second order boundary marked Z. This dissociation has been discussed in an earlier paper (12). The small triangular twinned region is indicated with the

subscript 3. The second order boundary plane is $(221)_3/(221)_2$, $(110)_m$, and this boundary contains a zig-zag arrangement of white dots faceted on the $(111)_3$ and $(111)_2$ planes with a periodicity of 1.15nm. These local periodicities and symmetries can be determined unambiguously since they are independent of the imaging conditions and transfer function of the microscope.

When odd numbered rings are joined symmetrically to form the dislocation core shown in figure 1, the ends of the core, marked E, are necessarily "pointed". Two cores cannot be joined directly together but must be connected by two six-fold rings as in figure 2, forming a unit A which is packed at maximum density in the $\Sigma=19$ structure. As Hornstra stated, there are two logical options when attempting to model a boundary with a higher misorientation angle than 26.53° , which he illustrated with the $\Sigma=9$ models of figure 3(a) and (b). The first model, figure 3(a), consists of two sets of $a/2[110]$ edge dislocations arranged in a zig-zag fashion and labelled B and C in the diagram. In the alternative model, figure 3(b), a dislocation with Burgers vector $a[110]$ has been created by interposing a six membered ring between the five and seven membered ones, forming a repeating unit labelled D. Note that this six membered ring is in the boat shaped configuration which is found in coherent first order twin boundaries. This model can be therefore be interpreted as an array of edge dislocations in a coherent first order twin boundary. The BC model, figure 3(a), can also be visualized in the same way, although it is not as obvious in this case. This point will be discussed in more detail below.

The zig-zag appearance of the $\Sigma=9$ boundary in figure 4 indicates that the BC sequence of figure 3(a) is more likely. This conclusion is in agreement with the findings of Krivanek et al (13), Papon et al (14) and Bourret et al (15) with regard to $\Sigma=9$ boundaries in germanium, although Bourret suggests that segregation of impurities to the interface may cause variations in the structure. In addition, the structure in figure 3(a) is more plausible from simple energetic considerations since the elastic energy per unit area of a symmetric tilt boundary is at a minimum when the ends of the extra half planes of atoms that terminate at the boundary (i.e. the dislocations) vary in spacing as little as possible. Examination of figures 3(a) and (b) shows that this criterion favors the BC sequence.

The $\Sigma=27$ model can be constructed using either an ABAC structural unit combination, figure 5(a), or an AAD combination, figure 5(b). The micrograph of the $\Sigma=27$ boundary in figure 4, which is reproduced at a higher magnification in figure 6(a), has the same repeat pattern as the faceted ABAC structure, and there is good correlation between large rings in the model and large dots in the image. The dotted line in figure 5(a) indicates $(111)_1$ and $(11\bar{1})_2$ facets. When figures 5(a) and 6(a) are superimposed, figure 6(b), there is good correlation between open channels and white dots, suggesting that the image is an accurate representation of the boundary structure, although this cannot be confirmed without multislice calculations.

Discussion

Several authors (Ashby, Spaepen, and Williams (7); Pond, Smith,

and Vitek (8), Sutton and Vitek (9); Frost, Spaepen and Ashby (10)) have described the structure of grain boundaries as a packing of a small number of (polyhedral) Bernal type atomic groups. This approach has largely been based on hard sphere modelling or computer simulated structures of grain boundaries in fcc metals where spherical potentials and central forces are assumed. There have been few attempts to extend this work to tetrahedrally coordinated materials with directional bonding, presumably due to the complexities of dealing with distorted sp^3 bonds. However, the concept of building up a boundary with a few simple units (i.e. dislocation cores) seems particularly suited to covalent structures. A system for modelling the structures of symmetric $\langle 110 \rangle$ tilt boundaries with tilt angles θ in the range 0° to 70.53° is presented.

Models for θ up to 38.94°

Symmetric boundaries with (110) median planes and values of θ up to 26.53° are modelled as an array of discrete $a/2[110]$ edge dislocations, unit A. Misorientations between 26.53° and 38.94° are modelled by combining structural units A, B, and C in a systematic manner, so that they are as evenly distributed as possible along the boundary. This is equivalent to adjusting the spacing between the dislocations so that the average spacing is given by $a/2[110] / (2\sin(\theta/2))$, and the variance of the spacing is a minimum. To preserve the symmetric nature of the boundary, the units B and C must occur alternately along the boundary. For example, a boundary whose repeating unit is AABAAC (a combination of $\Sigma=19$ and $\xi=27$) has a rotation angle of 29.70° corresponding to $\xi=137$, whereas a sequence of ABC or ABCACB ($\Sigma=27$ and $\xi=9$) gives a misorientation of 33.72° ($\xi=107$).

Final Report

ORIGINAL PAGE IS
OF POOR QUALITY

A simple method of determining the α and θ values for a particular combination is given. The vector \underline{d} joining the two ends of each structural unit is determined using a basis in which $(1,0)=a/2[110]_2$ and $(0,1)=a[001]_2$; thus for A $\underline{d}=1/2(1,3)$ and for BC $\underline{d}=(1,2)$. The repeat vector (r,s) (r and s integers) for the complete sequence of structural units making up the boundary is calculated and the value of Σ is found from $\Sigma=(r^2 + 2s^2)/w$ where w is 1 if r is odd, otherwise w is 2. The misorientation angle is found from $\tan(\theta/2)=r/2s$. The A,B and C units do not differ in their intrinsic structure, but rather in the way that they are joined together and the local distortions they impose on the lattice. The local Burgers vectors (16) of units A,B and C are $a/2[110]_m$, $a/2[110]_1$ and $a/2[110]_2$ respectively. These local Burgers vectors can be determined by considering which crystal contains the five and seven membered atom rings which constitute the dislocation core. The B and C units introduce translations of one crystal relative to the other at the boundary equal to their local Burgers vectors projected onto the boundary plane. For a $\Sigma=27$ boundary, these translations are equal and opposite, as is apparent in figure 5(a) where nearest neighbour A units have undergone equal but opposite shears. To minimize the energy of this alternating shear field, there is a rigid body translation of one crystal relative to the other, away from the coincidence position, of half the shift produced by a B (or C) unit. The shift produced by each B unit in the $\Sigma=27$ structure is $a/27[115]_1$, which is a DSC vector of the $31.59^\circ =27$ misorientation. The $\Sigma=27$ boundary plane contains screw axes half way between each (110) atomic plane. The $\Sigma=9$ boundary plane, figure 3(a), is a glide plane. Other boundaries with these symmetries (e.g. AABAAC, $\Sigma=137$ has glide symmetry) can be analyzed in the same way.

Less symmetric configurations (e.g. ABC, $\Sigma=107$) have more complex short range stress fields that are beyond the scope of the present paper.

Models for θ between 38.94° and 70.53°

The extension of the modelling system up to $\theta=70.53^\circ$, the first order twin orientation, is achieved by introducing the boat shaped six membered ring, T, into the $\Sigma=9$ structure of figure 3(a). This structure consists of alternating five and seven membered rings. The junctions between the five and seven rings have two different configurations, one symmetrical and the other asymmetrical. Only the symmetrical configuration can accommodate the T unit whilst still maintaining tetrahedral bonding. The structural model in figure 7 is created by placing one T unit in each symmetrical position. This structure contains two types of five and seven membered ring combinations, labelled G and H, which differ from units B and C. As more T units are added to the structure 7, the boundary misorientation increases. When the spacing of the G and H units becomes large, the boundary can be interpreted as isolated dislocations (G and H units) in a coherent first order twin boundary. Therefore, throughout the misorientation range from 38.94° to 70.53° , symmetric boundaries are modelled using G,H and T structural units distributed evenly along the boundary.

The d vectors of the T and GH units are $(1/2, 1/2)$ and $(1, 2)$ respectively. The GNHT sequence of figure 7 has a repeat vector of $(2, 3)$ and the model is therefore a $[332]\Sigma=11, 50.48^\circ$ boundary. The density of G and H units is a maximum for the $\Sigma=9$ structure and is

zero at the $\xi=3$ misorientation. Therefore, the reference lattice is twinned and the median plane is (111). Burgers circuits of the G and H units transferred to the twinned structure show that the Burgers vectors are $a/2[\overline{1}10]_1$ (G) and $a/2[\overline{1}\overline{1}0]_2$ (H). The G and H Burgers vectors are not normal to the common {111} boundary plane. However, twinning transforms $a/2[\overline{1}10]_2$ into $a/6[\overline{1}\overline{1}4]_1$, making the sum of the G and H Burgers vectors equal to $2a/3[\overline{1}\overline{1}1]_1$. As with the B and C units, the dislocations G and H introduce translations, at the boundary, equal to their Burgers vectors projected onto the boundary plane. These shifts are equal to $a/6[1\overline{1}2]$ at the twin orientation. The alternating shear field is apparent in figure 7 where neighbouring T units have undergone equal and opposite shears parallel to the boundary. The rigid body translation at the boundary which equalises the shears of the T units is $a/22[113]$, half a DSC vector of this structure. Bond bending in the crystals on either side of the boundary can absorb the shear strains without large increases in the energy of the structure. An alternative model for the $\xi=11$ boundary proposed by Papon et al (10) has a repeat unit of GHTT. The T units in this case are not sheared but an alternating tensile and compressive stress field is established normal to the boundary, due to the uneven spacing of the terminating planes of atoms. For this reason it is suggested that the GHTT structure may have a higher energy than the structure in figure 7.

In an exact analogy with the favored boundary model of Sutton and Vitek (13), small deviations from low coincidence values of θ are accommodated by varying the spacing of the primary dislocation by inserting "foreign" structural units at regular intervals. Any

departure from perfect regularity in the spacing of an array of primary dislocations can be analysed in terms of secondary dislocations. The Burgers vector of a secondary dislocation is the relative displacement of the two crystals due to a change in the spacing of the primary dislocations. Using an analysis similar to that of Bollmann (5), the matrix A describes the rotation of lattice 1 into lattice 2, and the displacement matrix T is given by $T=(I-A^{-1})$. If the vector \underline{x} is the change in the spacing of the primary dislocations, expressed in lattice 2, the Burgers vector of the secondary dislocation is given by $T\underline{x}$. For example a boundary composed of a repeating block of fifteen A units, one B unit, fifteen more A units and a C unit has a repeat vector of (16,47) and a deviation of .544 from the $\xi=19$ misorientation. Each π foreign π structural unit is associated with a grain boundary dislocation whose Burgers vector is $a/19[331]_1$.

Recent work on tilt boundaries in hard sphere fcc crystals (15) has shown that some symmetric boundaries, (particularly those with relatively long repeat lengths) could be constructed more densely when faceted. These boundaries usually had a dense plane in one crystal nearly parallel to a different dense plane in the other. In the case of the $\xi=27$ [552] boundary it was found that faceting on to $(111)_1/(110)_2$ and $(11\bar{1})_2/(110)_1$ planes reduced the excess volume by 28%. On each facet, the [111] and [110] planes were within 3.7° of being parallel. The boundary contained equal areas of $(110)_1$ and $(110)_2$ planes, consistent with a (110) median plane. This faceting is identical to that experimentally observed in figure 4.

Conclusions

Symmetric second and third order twin boundaries in silicon have been observed using high resolution TEM. Micrographs of a symmetric {221} $\Sigma=9$ boundary exhibited contrast features consistent with the zig-zag dislocation structure proposed by Hornstra (2) and similar to those reported in germanium (13-15). A model for a symmetric {552} $\Sigma=27$ boundary was constructed and found to have the same periodicity and faceted structure as an experimentally observed $\Sigma=27$ boundary. A system for modelling the structure of $\langle 110 \rangle$ tilt boundaries in tetrahedrally coordinated materials was developed based on the early work of Hornstra (1,2). Boundaries with (110) median planes and misorientations up to 70.53° were constructed using a repeating series of simple structural units.

Acknowledgements

Specimens were supplied by JPL. Central facilities operated by the Materials Science Center at Cornell were used to carry out part of this research.

References

1. J. Hornstra, *J. Phys. Chem. Solids* 5, 129 (1958).
2. J. Hornstra, *Physica* 25, 409 (1959).
3. M. H. Brodsky, S. Kirkpatrick and D. Weire in Tetrahedrally Bonded Amorphous Semiconductors, A.I.P. Conf. Proc. No. 20 (1974).
4. F. C. Frank in Symposium on plastic deformation of crystalline solids, p. 210, Carnegie Inst. of Technology (1950).
5. W. Bollmann, Crystal Defects and Crystalline Interfaces, p. 143 et seq. Springer-Verlag, Berlin (1970).
6. J. A. Kohn, *American Mineralogist* 41, 778 (1956).
7. M. F. Ashby, F. Spaepen and S. Williams, *Acta Met.* 26, 1647 (1978).
8. R. C. Pond, D. A. Smith and V. Vitek, *Acta Met.* 27, 235 (1979).
9. A. P. Sutton and V. Vitek, *Scripta Met.* 14, 129 (1980).
10. H. J. Frost, F. Spaepen and M. F. Ashby, accepted for *Scripta Met.*
11. A. Baghdadi and R. W. Gurtler, *J. Crystal Growth* 50, 236 (1980).
12. B. Cunningham, H. P. Strunk and D. G. Ast, *Scripta Met.* 16, 349 (1982).
13. O. L. Krivanek, S. Isoda and K. Kobayashi, *Phil. Mag.* 13, 931 (1977).
14. A-M. Papon, M. Petit, G. Silvestre and J-J. Bacmann in Grain Boundaries Semiconductors, p. 27, G. E. Pike, C. H. Seager and H. J. Leamy, Eds., Elsevier, N.Y. (1982).
15. A. Bourret, J. Desseaux and C. B'anterruches, *Inst. Phys. Conf. Series No. 60*, 9 (1981).
16. W. Bollmann, *Scripta Met.* 8, 1191 (1974).

Figure Captions

ORIGINAL PAGE IS
OF POOR QUALITY

Fig.1 Core structure of a $a/2 \langle 110 \rangle$ edge dislocation in the diamond lattice as proposed by Hornstra. The core configuration is symmetric and consists of one 5 and one 7 membered ring.

Fig.2 Model of a $\{331\}$, $\Sigma=19$, 26.53 degree tilt boundary according to Hornstra. This boundary has the highest misorientation that can be accommodated by a repetitive pattern of the edge dislocations shown in Fig. 1

Fig.3a First (of two alternative) models proposed by Hornstra for the structure of the $\{221\}$, $\Sigma=9$, 38.94 degree boundary. The boundary contains $a/2 \langle 110 \rangle$ edge dislocation arranged in a zig-zag pattern.

Fig.3b Second (of two alternative) models proposed by Hornstra for the structure of the $\{221\}$, $\Sigma=9$, 38.94 degree boundary. This boundary consists of a symmetric arrangement of $a \langle 110 \rangle$ dislocations.

Fig.4 Lattice fringe image of a 110 tilt boundary (incident electron beam parallel to tilt axis) at a magnification of $\times 6\,500\,000$. The section denoted by X is a $\{552\}/[552]$ symmetric third order twin boundary with a median boundary plane (110) . The boundary dissociates at Y into a coherent first order twin boundary and a symmetric second order boundary, denoted by Z.

ORIGINAL PAGE IS
OF POOR QUALITY

Fig.5a Schematic representation of the $\Sigma=27$ boundary, constructed of with a repeating group unit ABAC. For details see text.

Fig.5b Alternative version of the $\Sigma=27$ boundary, consisting of a repeating group unit AAD. For details see text.

Fig.6a Experimental micrograph of $\Sigma=27$ boundary. Magnification $\times 3000000$.

Fig.6b Superposition of the experimental micrograph of Fig. 6a and the schematic representation of the boundary with ABAC repeating groups (Fig. 5a).

Fig.7 Schematic representation of a [332] $\Sigma=11$, 50.48 degree tilt boundary consisting of GTHT repeating group unit. The boundary contains a rigid body translation $a/22[113]$. For more details see text.

ORIGINAL PAGE IS
OF POOR QUALITY

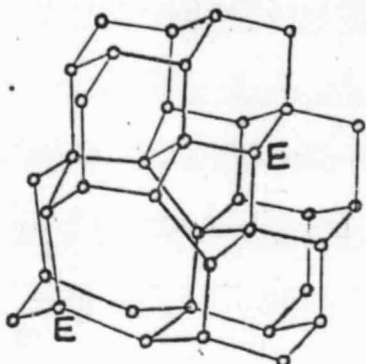


Fig.1

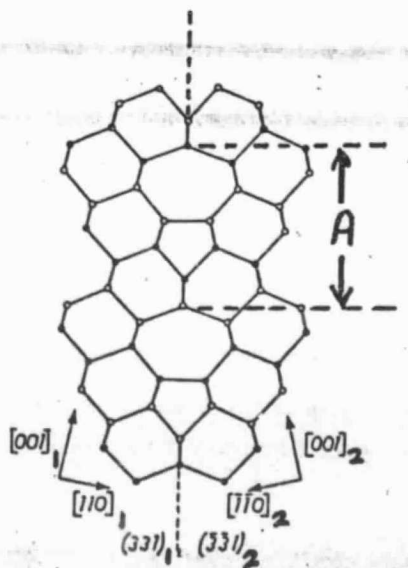


Fig.2

ORIGINAL PAGE IS
OF POOR QUALITY

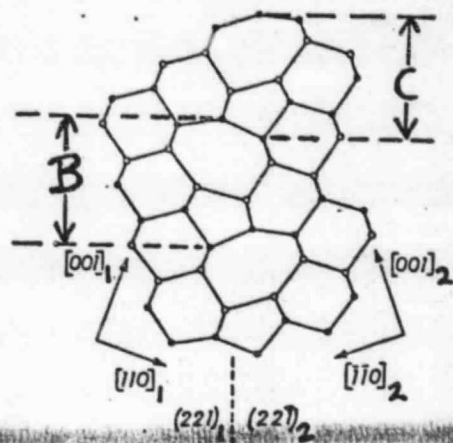


Fig. 3a

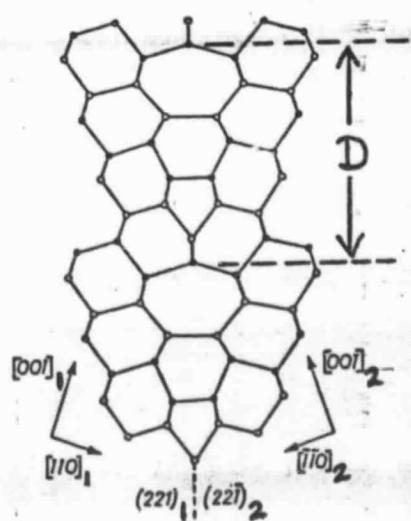


Fig. 3b

ORIGINAL PAGE IS
OF POOR QUALITY

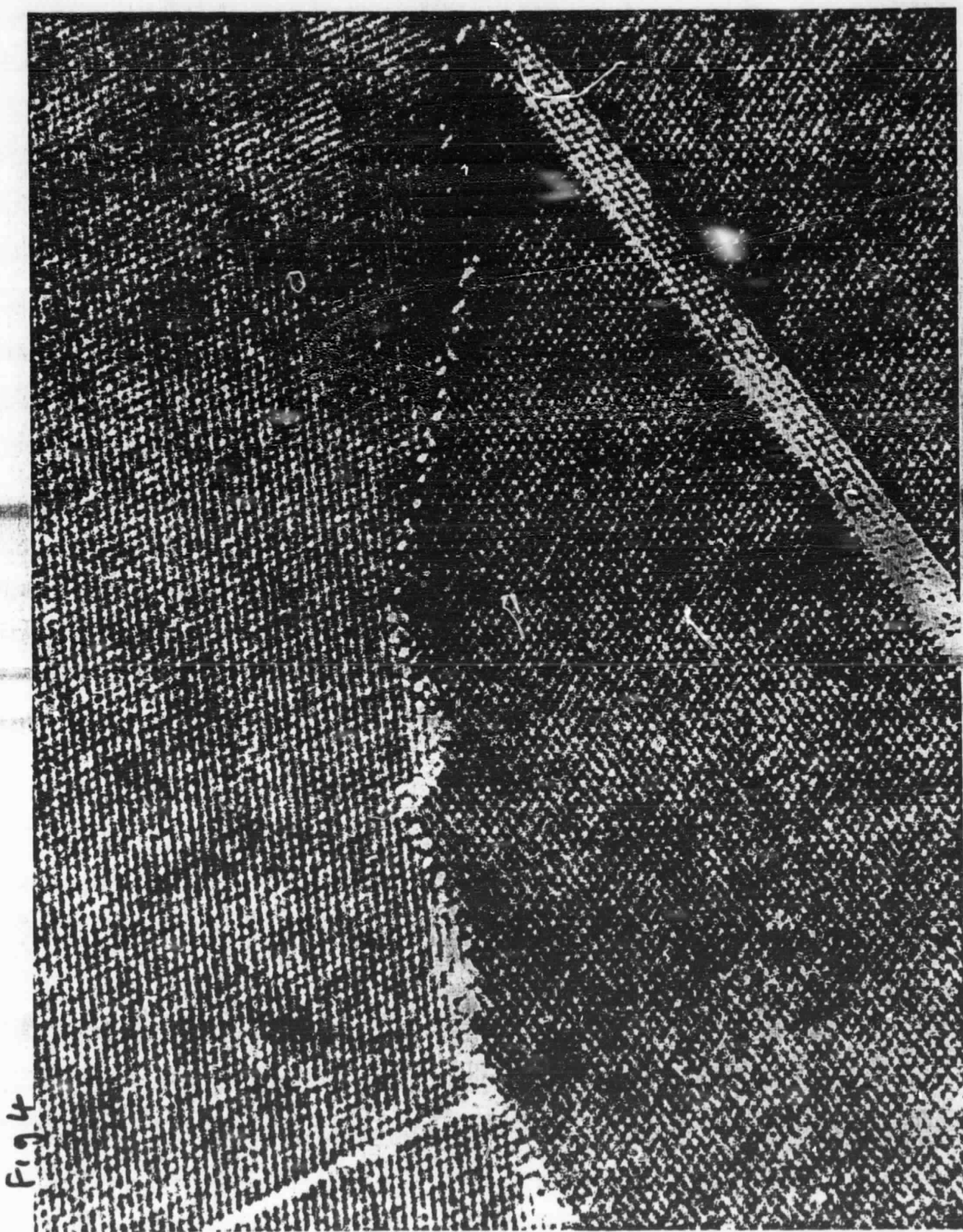


Fig 4

Magnification x 6 500 000

ORIGINAL PAGE IS
OF POOR QUALITY

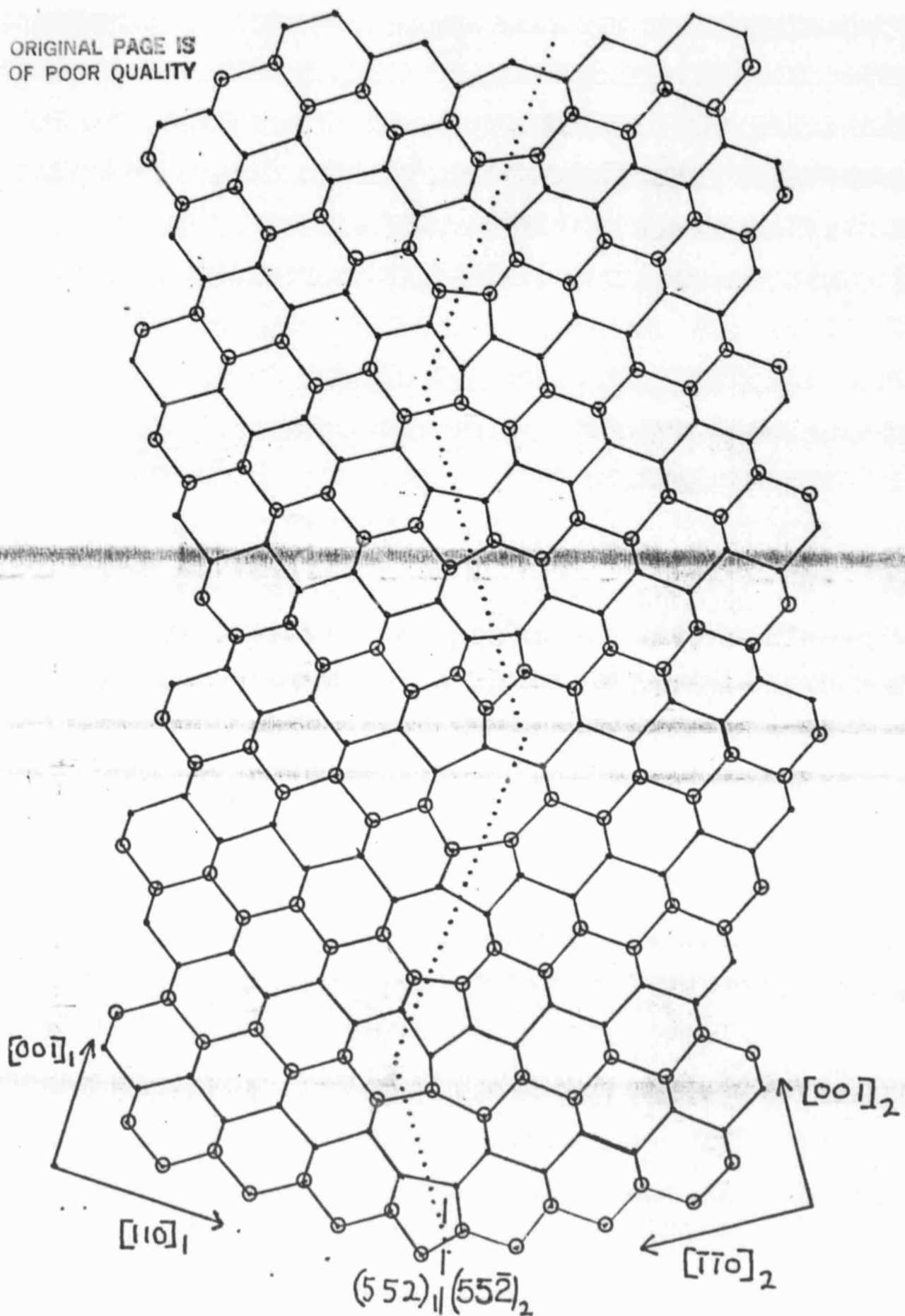


Fig. 5(a)

ORIGINAL PAGE IS
OF POOR QUALITY

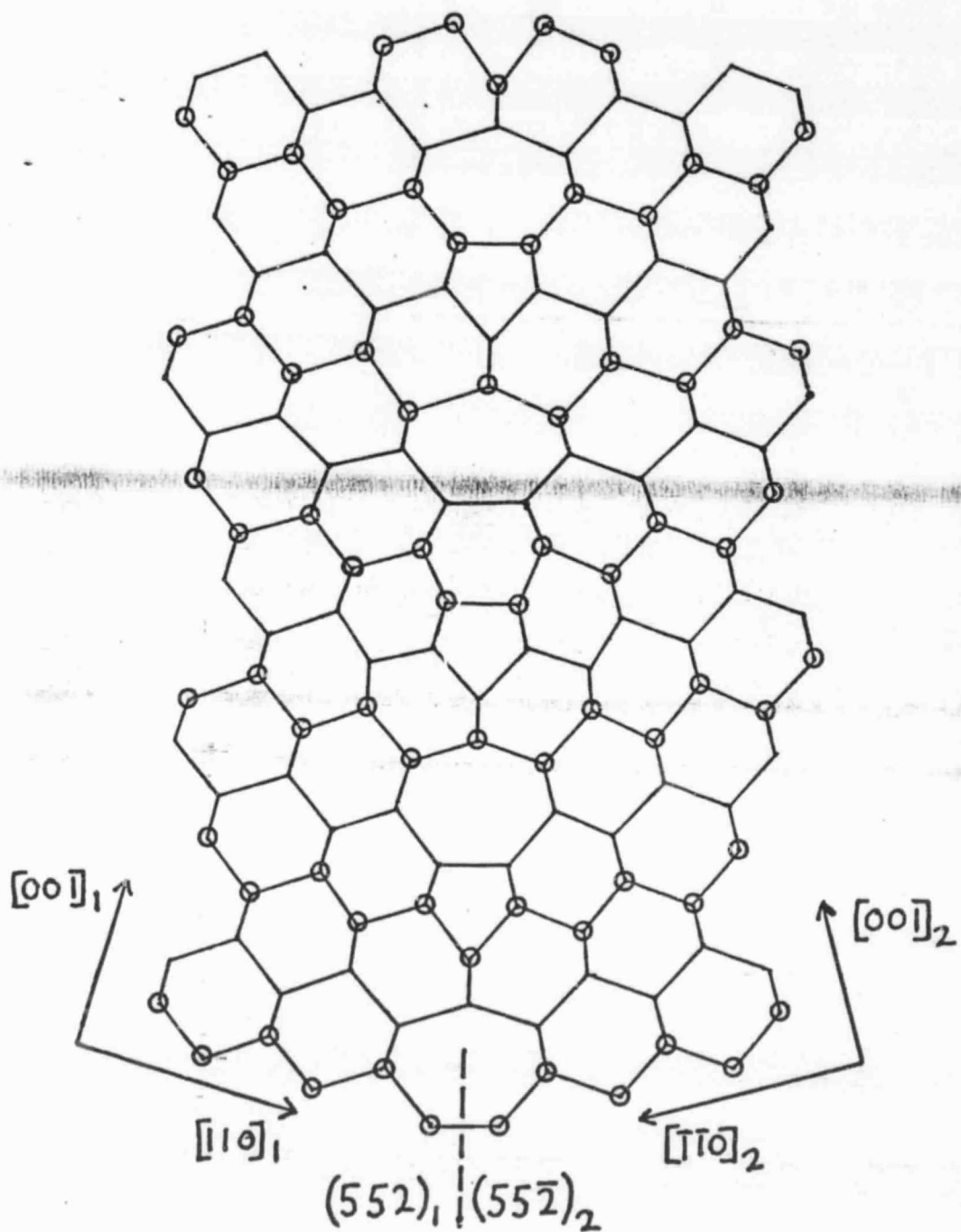


Fig. 5(b)



ORIGINAL PAGE IS
OF POOR QUALITY.

Fig. 6(a)

ORIGINAL PAGE IS
OF POOR QUALITY

ORIGINAL PAGE IS
OF POOR QUALITY

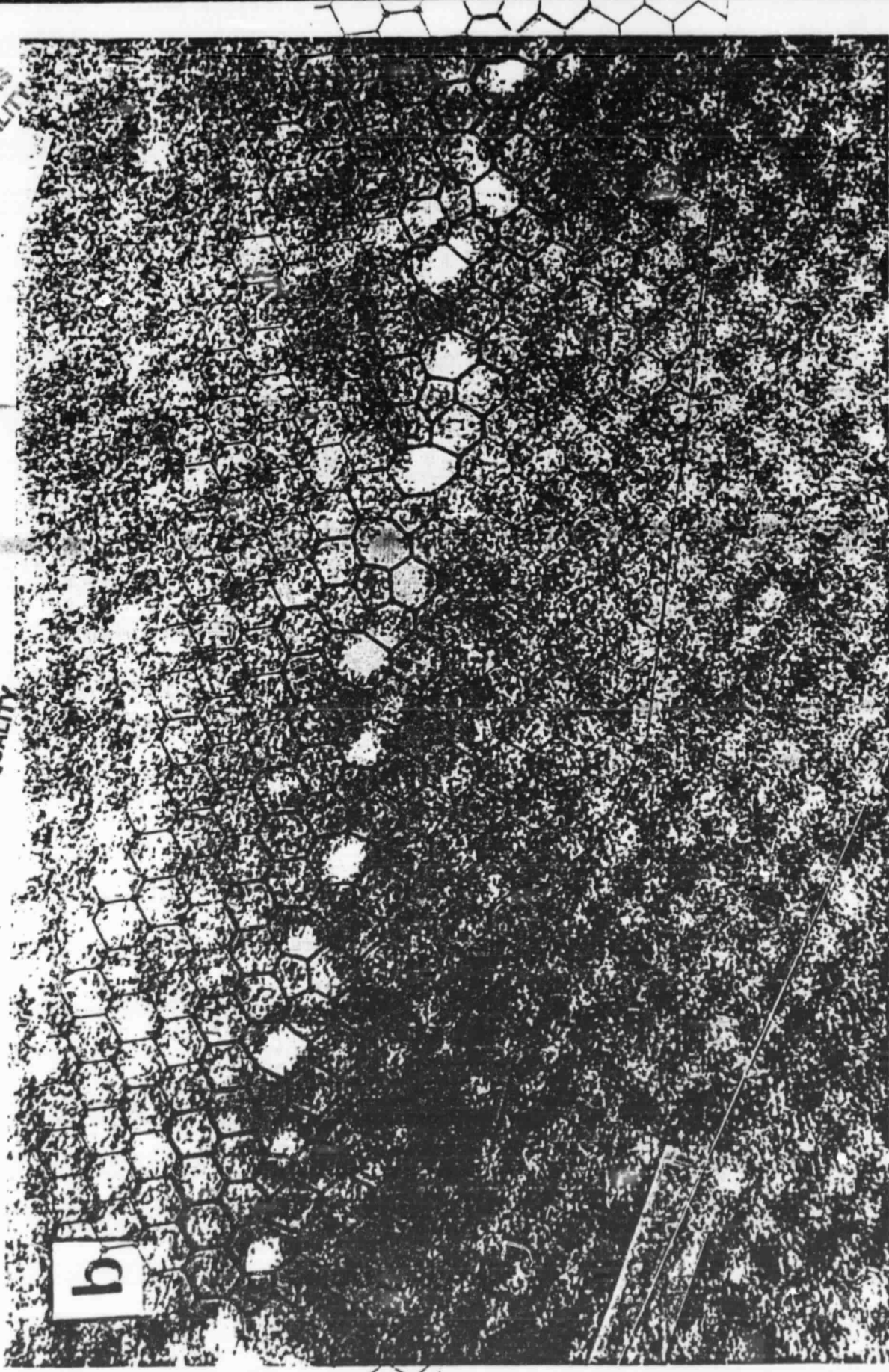


Fig 6b

ORIGINAL PAGE IS
OF POOR QUALITY

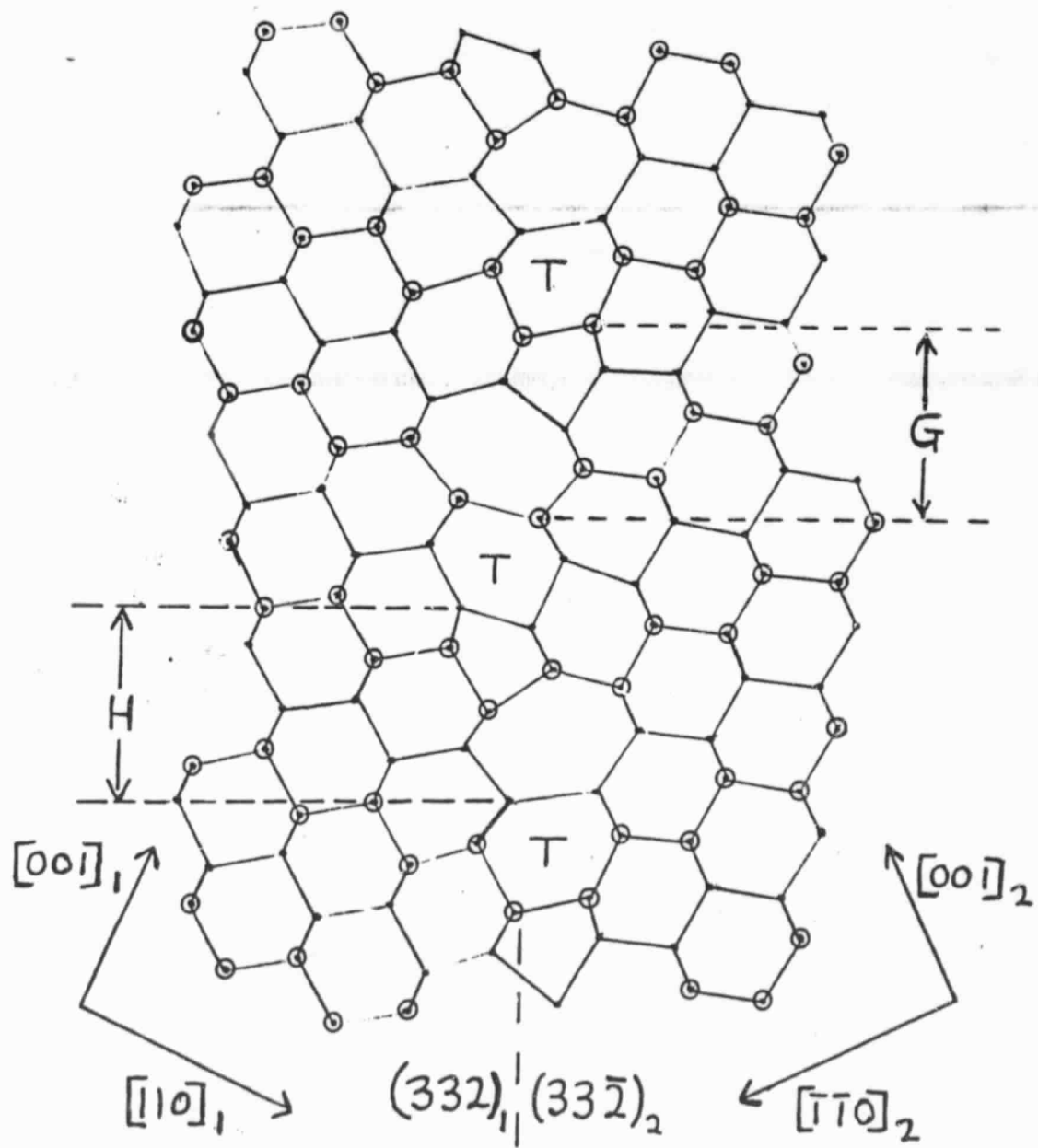


Fig. 7